



Biofuel production via transesterification using sepiolite-supported alkaline catalysts



Nebahat Degirmenbasi^{a,*}, Nezahat Boz^b, Dilhan M. Kalyon^c

^a Gazi University, Faculty of Sciences, Department of Chemistry, 06500 Teknikokullar, Ankara, Turkey

^b Gazi University, Faculty of Engineering, Department of Chemical Engineering, 06570 Maltepe, Ankara, Turkey

^c Department of Chemical Engineering and Materials Science, Stevens Institute of Technology, Hoboken, NJ 07030, USA

ARTICLE INFO

Article history:

Received 14 October 2013

Received in revised form 3 December 2013

Accepted 6 December 2013

Available online 16 December 2013

Keywords:

Biodiesel

FAME

Transesterification

Sepiolite

Potassium carbonate

ABSTRACT

Transesterification of oil to biodiesel was carried out using alkaline catalysis supported by sepiolite – a naturally-porous hydrated magnesium silicate with the highest surface area among all clay minerals. The catalyst particles, prepared by loading 10–50 wt.% of K_2CO_3 into sepiolite, followed by calcination at 773 K, were found to be very active in the catalysis of the transesterification reaction of canola oil with methanol. The purities of the biodiesel products were assessed via ATR-FTIR and 1H NMR and found to readily surpass the 96.5% purity requirement of the European EN standard 14103. The biodiesel yield was characterized as a function of the transesterification reaction time, the methanol to oil molar ratio, reaction temperature and catalyst concentration. Methyl ester yields of around $98.5 \pm 0.6\%$ could be obtained using sepiolite supports loaded with 40 and 50 wt.% K_2CO_3 . The testing of the recovered K_2CO_3 (50%)/sepiolite catalyst particles for their reusability and stability indicated that the initial catalytic activity of the catalyst could be maintained for at least five reaction cycles. This unusual maintenance of the activity of sepiolite supported catalysts is possibly associated with the minimization of the leaching of K_2O , occurring as a result of the special structure of sepiolite, that is unlike any other clay.

© 2013 Elsevier B.V. All rights reserved.

1. Introduction

Biodiesel (fatty acid methyl ester, FAME) is an attractive alternative to fossil based fuels on the basis of its biodegradability, non-toxicity and low C emission characteristics [1–3]. Biodiesel is generally produced using four different methods involving base-catalyzed transesterification, acid-catalyzed transesterification, enzyme-based transesterification and non-catalytic transesterification under supercritical alcohol conditions [4–8]. Transesterification of refined oils via homogeneous alkaline catalysts can lead to high quality biodiesel at relatively short reaction times in the range of 30–60 min [9]. However, such biodiesel production via homogeneous alkaline catalysts requires a costly sequence of production and purification steps since homogeneous alkaline catalysts do not tolerate the presence of moisture or free fatty acids [10]. Use of heterogeneous catalysts provides many

advantages in comparison to employing homogeneous catalysts including the recoverability and reusability of the catalyst particles and easier separation and purification of the glycerol (above 99%) and methyl esters [11–16].

The heterogeneous catalysts offered for the transesterification reactions of vegetable oils with methanol include the basic single metal oxides, i.e., calcium oxide [17–21], magnesium oxide [22] and strontium oxide [23]. Mixed metal oxides were also developed in order to enhance the basicity of the catalysts during the transesterification reaction of vegetable oils. Catalysts based on Al_2O_3 –SnO and Al_2O_3 –ZnO [24], Mg–La oxides [25], $CaMnO_3$, $Ca_2Fe_2O_5$, $CaZrO_3$, and $CaCeO_3$ [26] exhibit relatively high base strengths and can give rise to methyl ester yields of 80–99%.

The loading of potassium and sodium compounds into support materials has been widely applied to generate solid catalysts suitable for synthesis of biodiesel [6,27–29]. Alumina [30–33], nano alumina [15], calcium oxide [17,18,21], magnesium oxide [34,35], zinc oxide [27,36], zeolite [37], silica [38], dolomite [39] and bentonite [16,40] were functionalized with sodium or potassium compounds and were used as effective catalyst support materials

* Corresponding author. Tel.: +90 312 2021138; fax: +90 312 2213202.

E-mail address: nebahatd@gazi.edu.tr (N. Degirmenbasi).

for the transesterification reaction of vegetable oils. The catalytic activities of potassium or sodium compounds incorporated into catalyst supports depend on the type of the carrier material, the K, Na loading levels and the pretreatment conditions [6,27–29].

Clays such as zeolite, dolomite, kaolin, and bentonite are abundant, inexpensive and have relatively high surface to volume ratios to allow them to serve as catalyst supports for the transesterification of oils with methanol to biodiesel [16,37,39–41]. However, in spite of exhibiting the highest surface area of all the clay minerals (about 300 m²/g) sepiolite has not been seriously considered as a catalyst support for transesterification. Unlike other clays, sepiolite is not a layered phyllosilicate but consists of an assembly of needle-like particles separated by parallel channels with typical dimensions of 4 Å × 12 Å. These particles form loosely packed and porous aggregates with an extensive capillary network to give rise to the high porosity of sepiolite and its low density. On the basis of its interesting structure sepiolite has been utilized as a catalyst support various catalytic reaction systems including methanation of CO₂ with H₂, synthesis of light olefins from CO₂ hydrogenation, purification of ammonia synthesis feed gas by methanation method, selection oxidation reaction [42] and glycerolizes of triolein with glycerol [43]. However, to our knowledge, there is only one earlier study focusing on immobilized pig pancreatic lipase on sepiolite for preparation of a glycerol free biofuel [44].

Biodiesel fuel quality is generally analyzed by gas chromatography (GC) [15,16]. In recent years high-field nuclear magnetic resonance (NMR) (both ¹³C and ¹H) and attenuated total reflection Fourier transform infrared (ATR-FTIR) spectroscopy method have been used as alternative methods in order to characterize the fatty acid content of biodiesel [45–47]. ATR-FTIR method was also used to detect the presence of soap in the biodiesel mixture [45]. NMR offers online monitoring of transesterification process and the ability to reduce the analysis time for the reactants and products of the transesterification reaction [47,48].

Here potassium carbonate loaded (between 10 and 50 wt.%) sepiolite-based heterogeneous catalysts were prepared and utilized for the synthesis of fatty acid methyl ester. The synthesized catalysts were characterized using X-ray diffraction (XRD), scanning electron microscopy (SEM)–energy dispersive spectroscopy (EDS) and N₂ adsorption–desorption surface area analysis, BET, techniques. Basic strengths and the basicity of the synthesized catalysts were evaluated following the Hammett indicator procedure. The effects of K₂CO₃ over sepiolite ratio, the reaction temperature, methanol over oil and catalyst over oil ratios on the methyl ester yield were investigated as a function of reaction time. The recovery and reuse of the solid catalysts were also tested for transesterification reaction.

2. Experimental

2.1. Materials

The natural sepiolite used in this study was from Eskisehir region of Turkey [49–51]. Turkish sepiolite nodules were reported to exhibit superior physical properties especially related to purity, softness and whiteness [49–51]. K₂CO₃ and methanol (analytical-grade with a purity of 99.8 vol.%) was supplied by Riedel-de Haën. Methyl heptadecanate was obtained from Fluka and used for FAME analysis. The canola oil was purchased from a local vendor and its free fatty acid content was determined to be 0.085 wt.% following the AOCS Official Method Cd 3a-63 procedure [52]. The acid value of canola oil was calculated as 2.08 mg KOH g⁻¹.

2.2. Catalyst preparation

The sepiolite-based catalyst was prepared via the incipient-wetness impregnation method, which is a commonly used technique for the synthesis of heterogeneous catalysts. Sepiolite particles were crushed and ground and collected on 45 and 60 mesh sieves. Metal-containing aqueous solutions were added to the sepiolite particles. The volume of the solution that was added under vacuum matched the available void space of the sepiolite [15,16,32]. The water absorption of sepiolite particles was determined to be 2.09 ± 0.01 g per g of sepiolite. An aqueous solution of the K₂CO₃ was then prepared based on the water absorbance of sepiolite. The K₂CO₃ containing solution was pumped drop wise using a peristaltic pumps and was absorbed by the sepiolite particles.

K₂CO₃ impregnated sepiolite samples were prepared at 10, 20, 30, 40 and 50 wt.% K₂CO₃. For example, to prepare 50 wt.% K₂CO₃ based on sepiolite catalyst, 2.5 g of sepiolite sample was placed into a 250 ml flask held in an ultrasonic water bath. During impregnation vacuum was applied as the K₂CO₃ solution containing 2.5 g of K₂CO₃ was dissolved in 5.23 ± 0.01 g of deionized water, giving rise to 50% by weight of K₂CO₃ in K impregnated sepiolite catalyst. The impregnated sepiolite powder was dried in a vacuum oven at 373 K for 16 h. After the impregnation step sepiolite particles were calcined at 773 K in an air environment for 3 h to be ready for the transesterification reaction.

2.3. Catalyst characterization

BET (Brunauer–Emmett–Teller) surface areas of the synthesized catalysts were characterized according to the multipoint nitrogen adsorption–desorption method. Before each measurement, all samples were kept in an oven overnight at 393 K in order to eliminate possible effects of moisture absorption.

Basic strength and basicity of the synthesized catalysts were characterized using a Hammett indicator procedure described in detail by Boz et al. [15,16] and Xie et al. [53–55]. In this procedure about 300 mg of the sample was placed into one ml solution of Hammett indicators and then diluted with 10 ml of methanol. Two hours were allowed to elapse for equilibrium to be reached, as indicated by no additional changes of color. The basic strength is defined as being stronger than the weakest indicator, which exhibits a color change, however weaker than the strongest indicator that produces no color change. The Hammett indicators used in the analysis were bromothymol Blue (*H*_a = 7.2), phenolphthalein (*H*_a = 9.8), 2,4-dinitroaniline (*H*_a = 15.0) and 4-nitroaniline (*H*_a = 18.4). The basicity values (mmol/g) of the samples were evaluated by the method of Hammett involving the benzene carboxylic acid indicator (0.02 mol/l anhydrous ethanol solution) and titration until the color changed back to the original color [15,16,53–55].

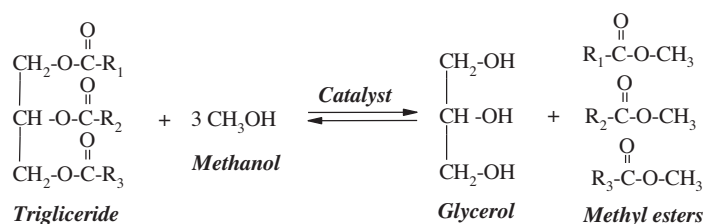
Powder X-ray diffraction (XRD) patterns of various samples were recorded on a Rigaku/D/MAX 2200 diffractometer with CuK_α radiation from a Cu X-ray tube running at 40 kV/40 mA at room temperature. All the measurements were performed over the Bragg angle (2θ) range of 5–75°.

SEM micrographs of the K₂CO₃ impregnated sepiolite particles were obtained using a Jeol JSM-6400 Scanning Microscope. The elemental chemical analysis of the samples was also characterized at room temperature using the energy dispersive X-ray spectroscopy (EDS) detector of the Jeol SEM.

2.4. The transesterification of canola oil to biodiesel

The transesterification of canola oil was carried out in a batch reactor, consisting of a 250 ml three-neck glass flask equipped with

a water-cooler condenser, temperature controlled magnetic stirrer, and a sampling port. Transesterification reaction is represented as;



where R_1 , R_2 and R_3 are long hydrocarbon chains. This reaction is reversible and hence, to shift the equilibrium toward right, excess alcohol is used [15,53–56]. The average molecular weight of canola oil was taken as 877 g/mol in the calculations for stoichiometry [57].

The reactor was initially filled with 50 g of canola oil, which was heated to the reaction temperature while stirring at 600 rpm. The reaction was timed to be initiated right after the mixture of alcohol and catalyst was added to the reactor. The effects of the K_2CO_3 over sepiolite ratio, the reaction temperature (298, 318, 333 and 338 K), molar ratio of methanol to oil (6:1–15:1), and catalyst/oil weight ratio (1–7 wt.%) on the conversion ratio of the triglycerides to biodiesel were investigated as a function of reaction time. All of the experiments were performed under atmospheric pressure and within 8 h of reaction time. The typical experiment involved the manual collection of about 2–3 ml of sample from the reactor at hourly intervals. The conversions achieved were determined not to be affected by the rate of rotation of the stirrer in the 400–1000 rpm range and the rotational speed of the stirrer was kept constant at 600 rpm during all of the reaction runs.

After the transesterification reaction, the catalyst was separated from the product mixture by filtration. Phase separation of the filtrate resulted in the isolation of the methyl esters and the glycerol within 24 h. The glycerol phase (bottom layer) and the methyl esters phase (top layer) exhibit different densities of 1.126 g/cm³ and 0.86, respectively and thus could be separated easily from each other. Excess methanol in the product was removed by evaporation to obtain pure biodiesel before chemical analysis.

Chemical analysis of the methyl esters was performed by an Agilent 6890 gas chromatograph (GC) equipped with a flame ionization detector and a capillary column CARBOWAX 20M. Sample preparation and GC analysis were carried out following European Standard of EN 14103 [58]. All data points reported in the study are reproduced in triplicate and 95% confidence intervals, determined according to Student's *t* distribution are reported.

Attenuated total reflection Fourier transform infrared (ATR-FTIR) spectroscopy and proton nuclear magnetic resonance (¹H NMR) methods were used for determining the compositions of canola oil and methyl esters. ¹H NMR spectra of canola oil and methyl esters were obtained on a Bruker ARX-400 spectrometer (Bruker, Rheinstetten, Germany) operating at 400 MHz (solvent: CDCl₃). A Nicolet 520 ATR-FTIR spectrometer with CsI beam splitter and DTGS detector was also used.

3. Results and discussion

3.1. Catalyst characterization

Physical properties of synthesized catalysts are reported in Table 1. The initial BET surface area of sepiolite was about 243 m²/g. After impregnation with the K_2CO_3 and calcination there was a significant reduction of the surface area, i.e., the surface and pores of the catalyst support were covered. The surface areas of K_2CO_3 doped catalyst particles decreased with increasing K_2CO_3 loading (Table 1). The BET surface areas of the catalysts synthesized using 30–50 wt.% of K_2CO_3 were similar. The low surface area and high basicity value of synthesized catalysts indicated that most of the basic sites remained within the core, interior region of the catalyst. This should allow more methanol and triglyceride to diffuse into the interior region of the catalyst. Thus, both the interior basic sites as well as the surface basic sites of the catalyst could be exploited for the transesterification reaction.

Nitrogen adsorption–desorption isotherms obtained with sepiolite and K_2CO_3 impregnated with different concentrations of K_2CO_3 , following calcination at 773 K for 3 h, are shown in Fig. 1. The nitrogen adsorption isotherms of sepiolite showed the typical Type II isotherm. On the other hand, the nitrogen adsorption isotherms of the synthesized catalysts exhibited the typical Type III isotherm, to indicate that the K_2CO_3 impregnated sepiolite catalyst supports are macroporous and exhibit a low energy of adsorption [59]. The capillary condensation of N₂ was observed at the relative range of 0.85 and 0.95. The pore size distributions of the materials used in this study are shown in Fig. 2. Most of the pores are in the 1–100 nm size range.

X-ray diffraction pattern of sepiolite, K_2CO_3 and catalysts with different K_2CO_3 loadings (10–50 wt.%) are shown in Fig. 3. XRD pattern of sepiolite particles exhibited the typical diffraction peaks at $2\theta = 7.54^\circ$, 19.94° , 21.30° , 23.42° , 26.38° , 27.38° , 34.76° , 37.54° and 40.4° . The results indicate that the sepiolite sample used in this study is mostly sepiolite on the basis of the 2θ values reported by others who have also utilized sepiolite samples from Eskisehir region of Turkey [60–62]. Upon K_2CO_3 impregnation, the typical K_2CO_3 patterns were observed at the Bragg angles, $2\theta = 27.06^\circ$, 30.74° , 33.16° , $38.68.0^\circ$, 42.16° , 43.68° , 46.34° , 49.14° and 67.52° . An additional K_2O phase appeared clearly in the diffraction patterns upon K_2CO_3 loading. The peaks associated with the K_2O phase are

Table 1
Physical properties of sepiolite and K_2CO_3 impregnated sepiolite catalysts.

		BET area (m ² /g)	Basic strength (H.)	Basicity (mmol/g) Standard error ± 0.05
1	Sepiolite	242.6	<7.2	0.15
2	K_2CO_3 (10%)/sepiolite	39.3	7.2 < H < 9.8	0.24
3	K_2CO_3 (20%)/sepiolite	20.1	9.8 < H < 15	0.44
4	K_2CO_3 (30%)/sepiolite	5.5	9.8 < H < 15	0.45
5	K_2CO_3 (40%)/sepiolite	4.4	9.8 < H < 15	2.72
6	K_2CO_3 (50%)/sepiolite	4.1	9.8 < H < 15	2.73

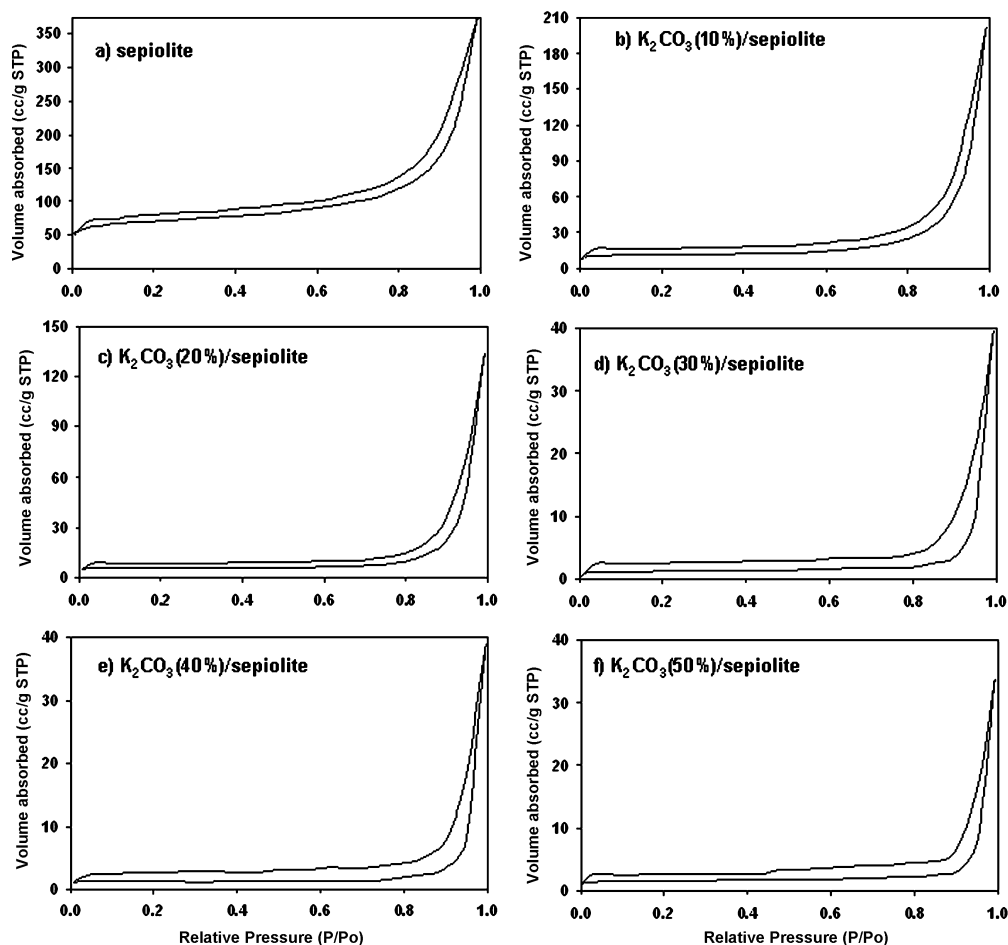


Fig. 1. Nitrogen adsorption–desorption isotherms of sepiolite, K_2CO_3 and sepiolite catalysts impregnated with different potassium carbonate loading levels (10–50 wt.%) upon calcination and prior to transesterification reaction.

observed at $2\theta = 30.0^\circ$, 42.04° and 53.4° . The intensities of these peaks increased with increasing K_2CO_3 content as expected.

Fig. 4 shows the typical SEM–EDS micrographs of sepiolite, and K_2CO_3 doped sepiolite catalyst particles. The typical fibrous morphology of sepiolite structure is observed as shown in Fig. 4a. The intensities of the peaks associated with the K content of the sepiolite surface increased significantly with increasing K_2CO_3 loading in the EDS spectrum (Fig. 4b and c). However, the intensities of

the Si and Mg peaks decreased with increasing K_2CO_3 content as expected. EDS analyses of the sepiolite surface and synthesized catalyst particles are also reported in Table 2. Each datum reported is the average value determined from three locations on the catalyst surface. Sepiolite is a Mg-rich clay mineral of trioctahedral type with a specific crystalline organization in channels and a typical unit cell formula for sepiolite is $Mg_8Si_{12}O_{30}(OH)_4(OH_2)_4 \cdot 8H_2O$

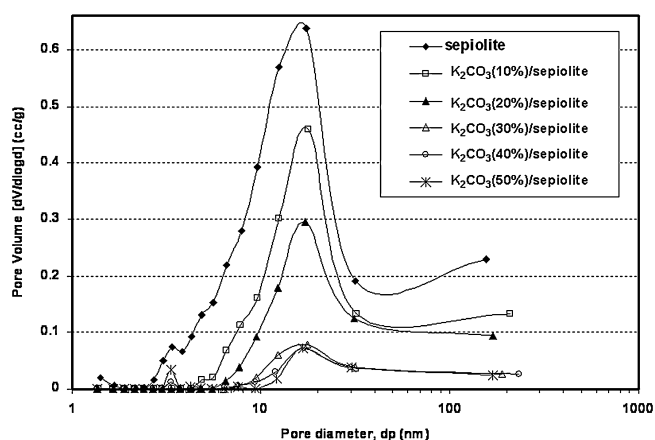


Fig. 2. Pore size distributions of sepiolite, K_2CO_3 and sepiolite catalysts impregnated with different potassium carbonate loading levels (10–50 wt.%) upon calcination and prior to transesterification reaction.

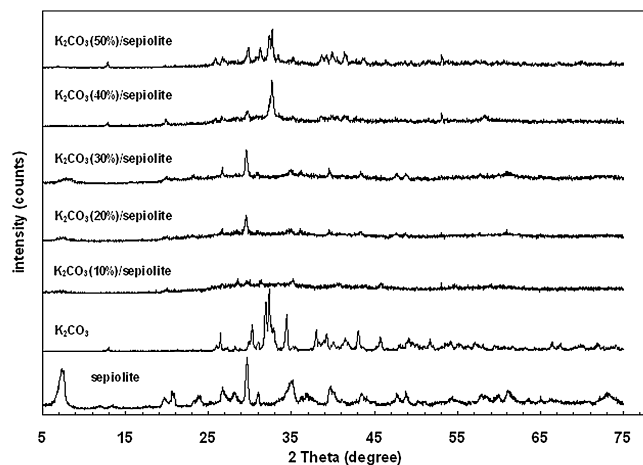


Fig. 3. XRD patterns of sepiolite, K_2CO_3 and sepiolite catalysts impregnated with different potassium carbonate loading levels (10–50 wt.%) upon calcination and prior to transesterification reaction.

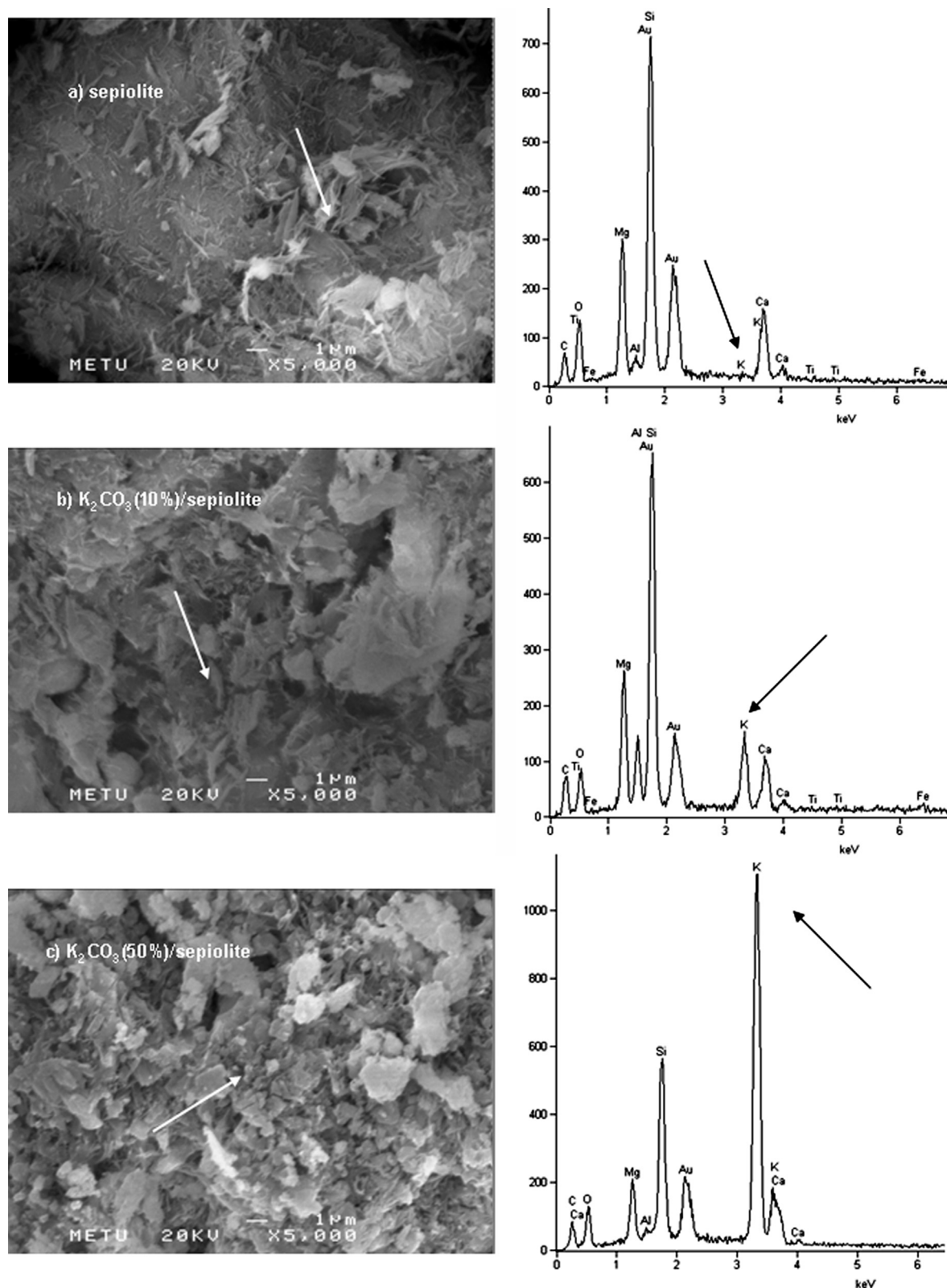


Fig. 4. SEM photographs with EDS spectrum of (a) pure sepiolite; (b) K_2CO_3 (10%)/sepiolite; and (c) K_2CO_3 (50%)/sepiolite prior to transesterification reaction.

[60–62]. As expected on the basis of this empirical formula, Si, Mg, Al, K, Ca and Fe are observed during EDS analysis. The K content of sepiolite prior to impregnation process is 0.19 wt.%. The results of the elemental analyses are very similar for K_2CO_3 loading levels of 40% and 50%. For example, the K contents of the sepiolite

surfaces impregnated with 40 and 50 wt.% K_2CO_3 are 31.09 and 31.12 wt.%, respectively. The relatively high K contents achieved at 40% and 50% loading levels of K_2CO_3 suggests that the process of loading K_2CO_3 into sepiolite could be successfully carried out.

Table 2
EDS analysis of the surfaces of sepiolite prior to and after the impregnation with K_2CO_3 .

Element	Weight (%)					
	Sepiolite	K_2CO_3 (10%)/sepiolite	K_2CO_3 (20%)/sepiolite	K_2CO_3 (30%)/sepiolite	K_2CO_3 (40%)/sepiolite	K_2CO_3 (50%)/sepiolite
O	48.79	46.05	41.88	41.74	41.45	41.46
Mg	12.58	12.07	11.33	8.55	7.75	7.74
Al	0.89	0.73	0.68	0.51	0.34	0.35
Si	26.87	26.11	24.4	18.87	16.26	16.24
K	0.19	7.22	16.62	27.07	31.09	31.12
Ca	10.2	7.36	4.72	2.91	2.78	2.77
Fe	0.48	0.46	0.37	0.35	0.33	0.32

3.2. Transesterification reaction

Effects of K_2CO_3 loading on the yield of methyl ester are shown in Fig. 5. The transesterification reaction of oil with methanol was carried out using a methanol/oil of 6/1, 3 wt.% of catalyst, at a reaction temperature of 338 K and reaction time of 8 h. The yield of methyl ester increases significantly with increasing K_2CO_3 loading and reaches an asymptotic conversion level between 40% and 50%, i.e., reaching $98.5 \pm 0.6\%$ at 50 wt. by weight of K_2CO_3 . The biodiesel yields which could be achieved at K_2CO_3 loading levels of 40–50% satisfy the biodiesel purity requirements of the European EN standard (EN-14103) which dictates that the purity of biodiesel should be at least 96.5% [58].

Table 1 indicates that the basicity of the synthesized catalysts varies significantly in a step manner with the K_2CO_3 loading. The basicity values of the catalyst particles loaded with 40% and 50% of K_2CO_3 (which provide the greatest biodiesel yields) are significantly greater than catalysts with lower concentrations of K_2CO_3 , i.e., $\leq 30\%$, indicating that the basicity plays a significant role in determining of the biodiesel yield. The basicity values of the catalyst supports with 40% and 50% of K_2CO_3 loading are similar at around 2.72–2.73 and the biodiesel yields reach asymptotic values of around 98.5% at these loading levels. This observed relationship between basicity and the biodiesel yield is consistent with our previous studies [15,16] and the earlier findings of Xie et al. [53–55]. Another factor of interest for the biodiesel yield would be the formation of new K_2O phase on the catalyst surface (Fig. 3). The XRD patterns of the catalyst particles with different loading levels of K_2CO_3 point out that there is a reduction in the formation of the K_2O phases with the decreasing of the K_2CO_3 loading level. Consequently, it is expected that the formation of the Si–O–K and Mg–O–K surface groups which serve as the active sites for the transesterification reaction of canola oil with methanol, would diminish accordingly, thus decreasing the yield of the biodiesel. The similarities in the elemental compositions of catalyst particles at 40% and

50% loading levels of K_2CO_3 reported in Table 2 are again indicative that the yield behaviors of catalyst particles at these two loading levels would be similar (noting that the basicities were also similar as shown in Table 1).

The effects of the other variables which can affect the methyl ester yield during the transesterification reaction, including the catalyst content, reaction temperature and the molar ratio of methanol to canola oil were investigated in conjunction with the 50 wt.% K_2CO_3 loaded catalyst. The samples were collected as a function of the reaction time at one-hour time intervals during reaction. The time dependent biodiesel yield data are reported in terms of the 95% confidence intervals determined according to Student's t distribution (Figs. 6–8).

For heterogeneously catalyzed transesterification system, the role played by the molar ratio of alcohol to oil (which is generally considered to be an important parameter in heterogeneously catalyzed transesterification reactions) is shown in Fig. 6. For the transesterification reaction stoichiometrically three moles of methanol are needed for each mole of triglyceride. However, generally significantly higher molar ratios are used, i.e., between 5:1 and 275:1 in order to enhance the rate of reaction [10,19–22,24,37,38,41,42]. Here, the transesterification reactions were carried out at molar ratios of alcohol to oil which were between 6:1 and 15:1. In these experiments the reaction temperature (338 K), the concentration of the catalyst particles in the batch reactor (3 wt.%) were kept constant. Methyl ester yields of around 80 wt.% were reached within the first hour at all methanol over oil

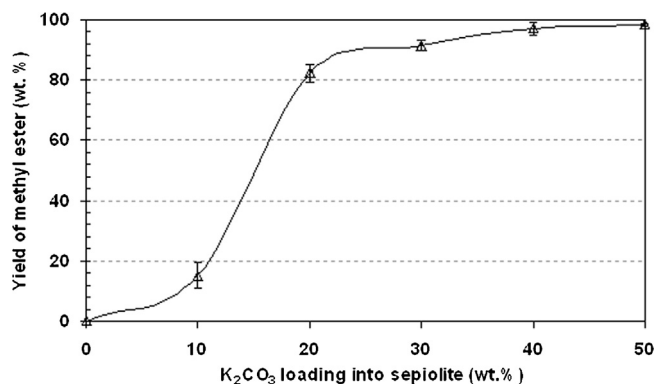


Fig. 5. Methyl ester yield vs the weight percent of K_2CO_3 loading into sepiolite (for methanol/oil molar ratio: 6/1, T : 338 K, catalyst amount: 3 wt.%, reaction time: 8 h). The standard error range is ± 0.24 –4.25.

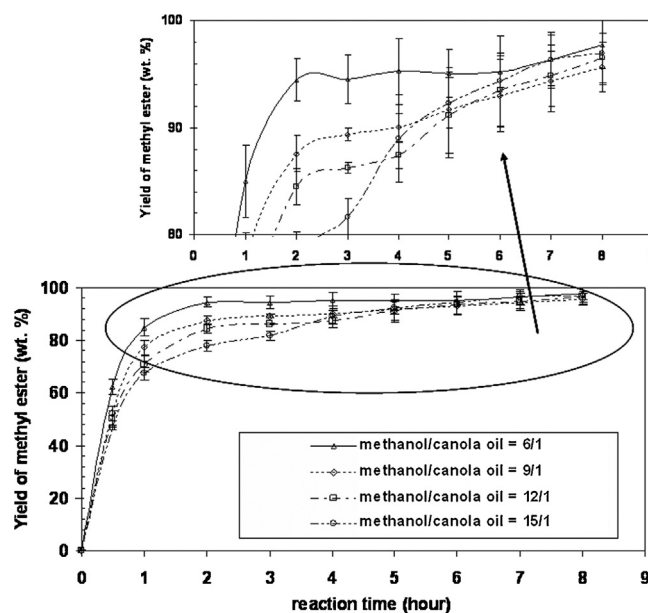


Fig. 6. Dependence of the methyl ester yield on the alcohol to oil molar ratio for synthesized K_2CO_3 (50%)/sepiolite catalyst (T : 338 K, catalyst amount: 3 wt.%, reaction time: 8 h) The standard error range is ± 0.33 –4.28.

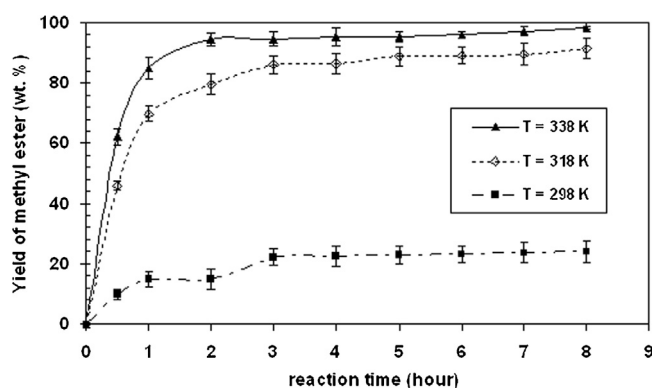


Fig. 7. Dependence of the methyl ester yield on the reaction temperature for synthesized $K_2CO_3(50\%)$ /sepiolite catalyst (for the methanol/oil molar ratio: 6/1, catalyst amount: 3 wt.%, reaction time: 8 h) The standard error range is ± 0.31 –5.19.

ratios. The methyl ester yields reached 90 wt.% at five hours. The yield results of Fig. 6 indicate that methanol/oil molar ratios that are greater than 6:1 do not increase further the methyl ester yield beyond what is achievable at the molar ratio of 6:1, i.e., the methyl ester yield of $98.5 \pm 0.6\%$. Furthermore, a relatively low ratio of alcohol to oil, such as 6:1, reduces the energy required for distillation.

The effects of the reaction temperature on the reaction rate and the biodiesel yield are shown in Fig. 7. The experiments were carried out at three temperatures (298, 318 and 338 K) while keeping constant the catalyst ($K_2CO_3(50\%)$ /sepiolite) concentration at 3 wt.% and the methanol to oil ratio at 6/1. The maximum temperature studied, i.e., 338 K, is the reflux temperature of methanol. The reaction rates and the biodiesel yields are significantly lower at 298, 318 K in comparison to those that could be achieved at 338 K. At 338 K the methyl ester yield reached $98.5 \pm 0.6\%$ at the end of the eight-hour reaction time.

The effects of the catalyst concentration on methyl ester yield were investigated for 50 wt.% K_2CO_3 loaded catalyst [$K_2CO_3(50\%)$ /sepiolite] as shown in Fig. 8. The weight ratio of the catalyst particles to canola oil was varied between 1.0% and 7.0%. The methyl ester yield increased with increasing catalyst concentration reaching a plateau value at a catalyst weight percent of about 3%. Increasing the catalyst concentration to be $>3\%$ did not lead to an increase of the methyl ester yield beyond what was achievable at 3 wt.%.

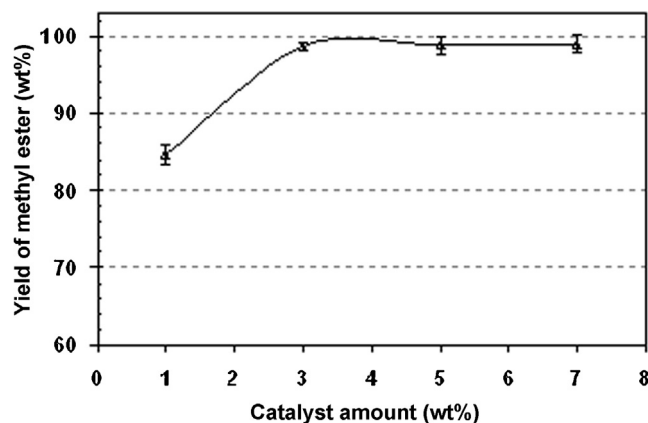


Fig. 8. The effects of the weight percent of the catalyst in the reaction mixture over synthesized $K_2CO_3(50\%)$ /sepiolite catalyst (for the methanol/oil molar ratio: 6/1, reaction temperature: 338 K, reaction time: 8 h). The standard error range is ± 0.33 –1.31).

Table 3

Characteristics bands of canola oil and related fatty acid methyl esters by using ATR-FTIR spectroscopy (the spectral region between 4000 and 400 cm^{-1}).

Canola oil (band position (cm^{-1}) and assignments)	Fatty acid methyl ester (band position (cm^{-1}) and assignments)
3006.92 cm^{-1} C=C–H stretching	3012.95 cm^{-1} C=C–H stretching
2936.21 cm^{-1} Aliphatic C–H stretching	2930.45 cm^{-1} Aliphatic C–H stretching
2847.82 cm^{-1} Aliphatic C–H stretching	2842.06 cm^{-1} Aliphatic C–H stretching
1737.09 cm^{-1} C=O stretching (ester)	1745.99 cm^{-1} C=O stretching (ester)
1468.98 cm^{-1} Aliphatic C–H in of plane stretching (for CH_2 and CH_3)	1466.08 cm^{-1} Aliphatic C–H in of plane bending (for CH_2 and CH_3)
1377.64 cm^{-1} Aliphatic C–H in of plane stretching (for CH_2 and CH_3)	1348.22 cm^{-1} Aliphatic C–H in of plane bending (for CH_2 and CH_3)
–	1427.77 cm^{-1} CH_3 asymmetric bending ($COO-CH_3$)
–	1195.01 cm^{-1} O– CH_3 stretching
1162.57 cm^{-1} C–O–C symmetric stretching	1174.38 cm^{-1} C–O–C symmetric stretching
1109.54 cm^{-1} O– CH_2 –C asymmetric stretching	–
726.52 cm^{-1} Aliphatic C–H out of plane bending (for $CH_2 > 4$)	714.74 cm^{-1} Aliphatic C–H out of plane bending ($CH_2 > 4$)

The biodiesel samples with a purity of $98.5 \pm 0.6\%$ and resulting from the transesterification reaction using 50 wt.% K_2CO_3 loaded sepiolite catalyst, 8 h of reaction time at 338 K, 3 wt.% catalyst and at 6:1 molar ratio of methanol/oil were characterized further employing ATR-FTIR (Fig. 9) and 1H NMR (Fig. 10) analyses. The ATR-FTIR spectra of canola oil and biodiesel exhibit similarities since both are fairly strong absorbers in the infrared region. Table 3 shows the characteristic bands of canola oil and fatty acid methyl within the spectral region between 4000 and 400 cm^{-1} . The major differences in the spectra arise at 1427.77 cm^{-1} which corresponds to CH_3 asymmetric bending for $COO-CH_3$ and at 1195.01 cm^{-1} which corresponds to O– CH_3 stretching band (Fig. 9b). The band observed at 1109.54 cm^{-1} corresponds to the O– CH_2 –C asymmetric stretching in the canola oil spectrum (Fig. 9a) which is not observed for methyl esters, as expected. These FTIR findings attest to the structure validation of the biodiesel produced in this study.

Fig. 10 shows the 1H NMR spectra of the canola oil and the methyl esters. Biodiesel in these analyses were made both before and after evaporation of excess methanol in the mixtures of methyl esters to demonstrate the effects of the methanol impurity in the biodiesel product spectra. Clear differences were observed. Fig. 10a shows the 1H NMR spectrum of the canola oil. The glyceridic protons of the canola oil are observed between 4.10 and 4.40 ppm (shown as G1) and at 5.25 ppm (shown as G2). The disappearance of these signal in the spectrum biodiesel sample verify the biodiesel structure (Fig. 10b and c). The large signal observed at 3.65 ppm (shown as M on the spectrum) corresponds to the methyl ester protons in the biodiesel sample. The olefinic protons bands ($-CH=CH-$) observed between 5.30 and 5.50 ppm and the bis-allylic protons ($-CH=CH-CH_2-CH=CH-$) bands between 2.70 and 2.90 ppm appear in both of the canola oil and biodiesel spectra. These NMR findings are consistent with the results of other studies carried out using different vegetables oils and corresponding methyl esters [47,48,63,64].

In conventional production of biodiesel, relatively high methanol concentrations are used. The maximum allowable concentration of methanol in pure biodiesel is specified in the European standard of EN 14214 to be 0.20% [65]. The characteristic peaks in the 1H NMR

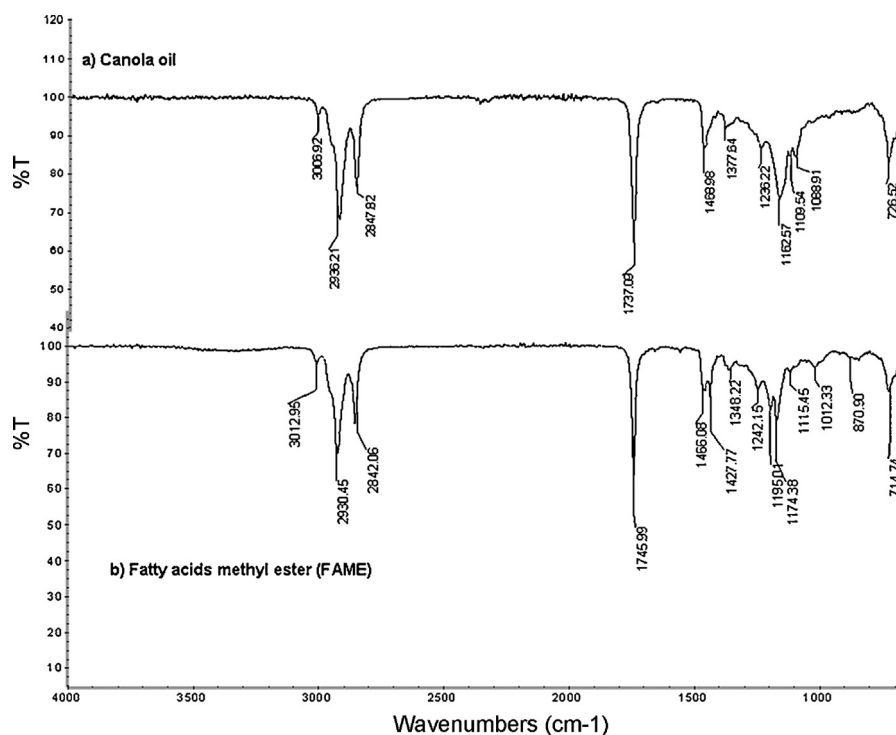


Fig. 9. ATR-FTIR results of canola oil and methyl esters obtained on K_2CO_3 (50%)/sepiolite catalyst (for the methanol/oil molar ratio: 6/1, reaction temperature: 338 K, reaction time: 8 h, and catalyst amount: 3 wt.%).

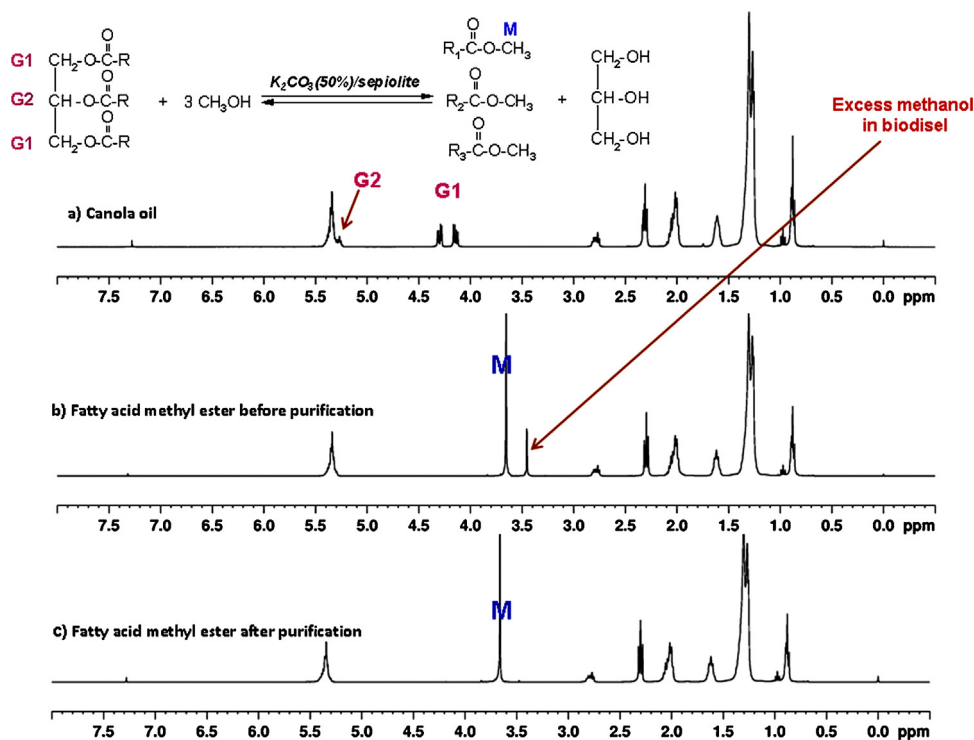


Fig. 10. ¹H NMR results of canola oil and methyl esters obtained on K_2CO_3 (50%)/sepiolite catalyst (for the methanol/oil molar ratio: 6/1, reaction temperature: 338 K, reaction time: 8 h, and catalyst amount: 3 wt.%).

for methanol are those of the OH stretching protons at 3.66 ppm and CH₃ stretching protons at 3.43 ppm [66]. The CH₃ stretching band of methanol was observed at 3.44 in our sample of biodiesel before purification (Fig. 10b). However, CH₃ stretching band of methanol

disappeared completely in the spectrum of biodiesel after purification (Fig. 10c). These NMR results again suggest that both canola oil and the synthesized biodiesel could be differentiated and biodiesel with acceptable purity could be produced.

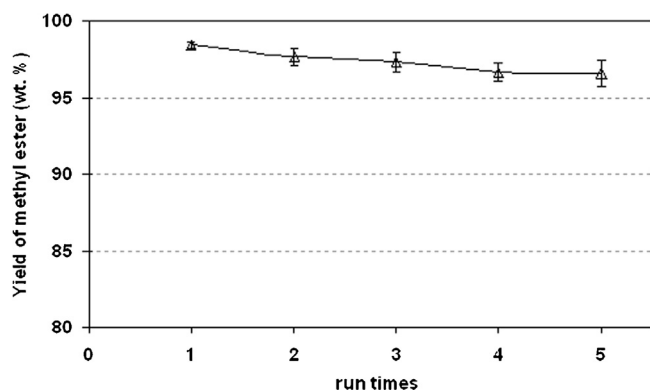


Fig. 11. The effects of reusability of the catalyst particles ($K_2CO_3(50\%)/\text{sepiolite}$ catalyst (under the methanol/oil molar ratio: 6/1, temperature: 338 K, reaction time: 8 h, catalyst amount: 3 wt.%, calcination temperature and time: 773 K and 3 h). The standard error range is $\pm 0.57\text{--}0.86$).

3.3. Stability and reusability of $K_2CO_3(50\%)/\text{sepiolite}$ catalyst

The stability and reusability of the catalyst are important for the commercializing of heterogeneous catalytic systems for use in manufacturing of biodiesel. The $K_2CO_3(50\%)/\text{sepiolite}$ catalyst particles were tested for their recoverability and stability. The transesterification reaction of oil with methanol was carried out multiple times under one constant set of operating conditions (methanol/oil: 6/1, catalyst amount: 3 wt.%, temperature: 338 K, reaction time: 8 h). Upon the completion of each cycle of the transesterification reaction the catalyst particles were filtered out, recovered, washed with methanol several times, re-calcined at 773 K for 3 h and then reused as the catalyst for the next reaction cycle. Fresh reaction mixtures of methanol and canola oil were used at each cycle.

The results pertaining to the methyl ester yield vs the number of recycling cycles are shown in Fig. 11, which indicate that the $K_2CO_3(50\%)/\text{sepiolite}$ catalyst maintained sustained activity even after being recycled five times. Only a small decrease of the methyl ester yield, i.e., from 98.5 ± 0.6 to $96.6 \pm 0.7\%$ was observed when the yields of the first and fifth cycles are compared. Generally, part of the K that is initially deposited onto the catalyst support can leach out of the catalyst particles during the reaction [15,16,33,40,67].

The observed lack of decrease of activity and associated maintainability of the biodiesel yield upon recycle and reuse of the catalyst particles possibly points to the special structure of sepiolite and the role its high porosity and surface to volume ratio plays. The structure of sepiolite is unusual in that it is characterized by quincunx-type geometry of talc-type sheets separated by parallel channels consisting of high aspect ratio, i.e., needle-like particles instead of the typical plate-like structures of other clays [http://www.ima-europe.eu/about-industrial-minerals/industrial-minerals-ima-europe/sepiolite]. The building blocks, i.e., the elongated particles of sepiolite containing relatively narrow-open channels with areas of around 40 \AA^2 , running along the axis of the particles, form an extensive capillary network to give rise to the high porosity of sepiolite [http://www.ima-europe.eu/about-industrial-minerals/industrial-minerals-ima-europe/sepiolite], while apparently making it difficult for the K_2O to leach out.

4. Conclusions

Catalytic activities of sepiolite supports that are impregnated with aqueous K_2CO_3 solutions catalysts were tested for the transesterification of canola oil with methanol. The reaction parameters included the temperature (298–338 K), methanol/oil ratios (6:1–15:1), reaction time (1–8 h), catalyst concentration in the

batch reactor (1–7 wt.%) and different K_2CO_3 loading levels into sepiolite (10–50%). Relatively high methyl ester yields around 98.5% could be obtained under the catalyst preparation and transesterification conditions of K_2CO_3 loadings of 40–50 wt.%, calcination temperature of 773 K, 8 h of reaction time at 338 K, 3 wt.% catalyst in the reaction mixture and methanol/oil molar ratio of 6:1. Such high yields of biodiesel are considered to be associated with the high surface to volume ratio of the sepiolite particles, the relatively high basicity of the catalyst surfaces ($2.72\text{--}2.73 \text{ mmol/g}$) and the high concentration of K groups. ATR-FTIR and ^1H NMR results verified the structure and the purity of biodiesel produced in this study. Recovery and reusability studies of the sepiolite supported catalyst particles revealed that the sepiolite-supported catalysts maintained their activities for at least five reaction cycles. This unusual recyclability indicates that sepiolite supports offer significant advantages in comparison to other clays in preventing the leaching of K_2O that is incorporated into the catalyst support, reflecting the special structure of sepiolite, which is unlike any other clay. Overall, sepiolite was found to be a suitable support material for the preparation of K supported biodiesel catalysts for the canola oil transesterification reaction, while offering significant advantages in recyclability of the catalyst particles.

Acknowledgements

The authors acknowledge the research funding provided by Gazi University under project number BAP-FEF-05/2008-06 and BAP-FEF-05/2009-31. The authors also thank the Central Laboratory and Department of Metallurgical and Materials Engineering of Middle East Technical University for BET, XRD Diffraction and SEM-EDS analysis.

References

- [1] Y.C. Sharma, B. Singh, *Renewable Sustainable Energy Reviews* 13 (2009) 1646–1651.
- [2] S.B. Lee, K.H. Han, J.D. Lee, I.K. Hong, *Journal of Industrial and Engineering Chemistry* 16 (2010) 1006–1010.
- [3] R. Alcantara, J. Amores, L. Canoria, E. Fidalgo, M.J. Franco, A. Navarro, *Biomass and Bioenergy* 18 (2000) 515–527.
- [4] S. Chongkhong, C. Tongurai, P. Chetpattananondh, *Renewable Energy* 34 (2009) 1059–1063.
- [5] M. Canakci, V. Gerpen, *Transactions of the American Society of Agricultural Engineers* 42 (1999) 1203–1210.
- [6] W. Du, Y. Xu, J. Zeng, D. Liu, *Biotechnology and Applied Biochemistry* 40 (2) (2004) 187–190.
- [7] K.R. Jegannathan, S. Sariah Abang, D. Denis Poncelet, E.S. Chan, P. Ravindra, *Critical Reviews in Biotechnology* 28 (4) (2008) 253–264.
- [8] H. He, T. Wang, S. Zhu, *Fuel* 86 (3) (2007) 442–447.
- [9] Y. Wang, S. Ou, P. Liu, Z. Zhang, *Energy Conversion and Management* 48 (2007) 184.
- [10] D.Y.C. Leung, X. Wu, M.K.H. Leung, *Applied Energy* 87 (2010) 1083–1095.
- [11] D.M. Alonso, R. Mariscal, R. Moreno-Tost, M.D.Z. Poves, M.L. Granados, *Catalysis Communications* 8 (2007) 2074–2080.
- [12] U. Schuchardt, R. Sercheli, G. Gelbard, *Journal of the Brazilian Chemical Society* 9 (1) (1998) 199–210.
- [13] S. Semwal, A.K. Arora, R.P. Badoni, D.K. Tuli, *Bioresource Technology* 102 (2011) 2151–2161.
- [14] E. Li, V. Rudolph, *Energy & Fuels* 22 (1) (2008) 145–149.
- [15] N. Boz, N. Degirmenbasi, D.M. Kalyon, *Applied Catalysis B: Environmental* 89 (2009) 590–596.
- [16] N. Boz, N. Degirmenbasi, D.M. Kalyon, *Applied Catalysis B: Environmental* 138 (2013) 236–242.
- [17] M.L. Granados, M.D.Z. Poves, D.M. Alonso, R. Mariscal, F.C. Galisteo, R. Moreno-Tost, J. Santamaría, J.L.G. Fierro, *Applied Catalysis B: Environmental* 73 (2007) 317–326.
- [18] X. Liu, H. He, Y. Wang, S. Zhu, X. Zhao, *Fuel* 87 (2008) 216–221.
- [19] M. Kouzu, T. Kasuno, M. Tajika, Y. Sugimoto, S. Yamanaka, J. Hidaka, *Fuel* 87 (2008) 2798–2806.
- [20] V.B. Veljkovic, O.S. Stamenkovic, Z.B. Todorovic, M.L. Lazic, D.U. Skala, *Fuel* 88 (2009) 1554–1562.
- [21] A. Kawashima, K. Matsubara, K. Honda, *Bioresource Technology* 100 (2009) 696–700.
- [22] T.F. Dossin, M.F. Reyniers, R.J. Berger, G.B. Marin, *Applied Catalysis B: Environmental* 67 (2006) 136–148.

- [23] X. Liu, H. He, Y. Wang, S. Zhu, *Catalysis Communications* 8 (2007) 1107–1111.
- [24] C.C.S. Macedo, F.R. Abreu, A.P. Tavares, M.B. Alves, L.F. Zara, J.C. Rubim, P.A.Z. Suarez, *Journal of the Brazilian Chemical Society* 17 (2006) 1291–1296.
- [25] N.S. Babu, R. Sree, P.S.S. Prasad, N. Lingaiah, *Energy & Fuels* 22 (2008) 1965–1971.
- [26] A. Kawashima, K. Matsubara, K. Honda, *Bioresource Technology* 99 (2008) 3439–3443.
- [27] W. Xie, H. Li, *Journal of Molecular Catalysis A: Chemical* 255 (2006) 1–9.
- [28] Y. Li, B. Ye, J. Shen, L. Wang, L. Zhu, T. Ma, D. Yang, F. Qiu, *Bioresource Technology* 137 (2013) 220–225.
- [29] S. Baroutian, M.K. Aroua, A.A.A. Raman, N.M.N. Sulaiman, *Fuel Processing Technology* 91 (11) (2010) 1378–1385.
- [30] G. Arzamendi, I. Campo, E. Arguiñarena, M. Sánchez, M. Montes, L.M. Gandía, *Chemical Engineering Journal* 134 (2007) 123–130.
- [31] S. Benjapornkulaphong, C. Ngamcharussrivichai, K. Bunyakiat, *Chemical Engineering Journal* 145 (2009) 468–474.
- [32] N. Boz, M. Kara, *Chemical Engineering Communications* 196 (2009) 80–92.
- [33] O. Ilgen, A.N. Akin, *Energy & Fuels* 23 (4) (2009) 1786–1789.
- [34] L. Wang, J. Yang, *Fuel* 86 (2007) 328–333.
- [35] X. Liang, S. Gao, H. Wu, J. Yang, *Fuel Processing Technology* 90 (2009) 701–704.
- [36] N. Boz, O. Sunal, *Journal of the Faculty of Engineering and Architecture of Gazi University* 24 (3) (2009) 389–395.
- [37] W. Xie, X. Huang, H. Li, *Bioresource Technology* 98 (2007) 936–939.
- [38] C. Samart, P. Sreetongkittikul, C. Sookman, *Fuel Processing Technology* 90 (2009) 922–925.
- [39] O. Ilgen, *Fuel Processing Technology* 92 (2011) 452–455.
- [40] F.E. Soetaredgo, A. Ayucitra, S. Ismadji, A.L. Maukar, *Applied Clay Science* 53 (2011) 341–346.
- [41] L.A.S. do Nascimento, R.S. Angélica, C.E.F. da Costa, J.R. Zamian, G.N. da Rocha Filho, *Applied Clay Science* 51 (2011) 267–273.
- [42] M.A. Hong-Tao, D. Guo-Cai, X. Li, L. Meng-Qing, C. Rong-Ti, H. Sen, X. Gen-Hui, *Journal of Natural Gas Chemistry* 8 (2) (1999) 93–104.
- [43] A. Corma, S. Iborra, S. Miguel, J. Primo, *Journal of Catalysis* 173 (1998) 315–321.
- [44] V. Caballero, F.M. Bautista, J.M. Campelo, D. Luna, J.M. Marinas, A.A. Romero, J.M. Hidalgo, R. Luque, A. Macario, G. Giordano, *Process Biochemistry* 44 (2009) 334–342.
- [45] C. Baroi, E.K. Yanful, M.A. Bergougnou, *International Journal of Chemical Reactor Engineering* 7 (2009), Article A72.
- [46] G. Knothe, J.A. Kenar, *European Journal of Lipid Science and Technology* 106 (2004) 88–96.
- [47] Y.G. Linck, M.N.M. Killner, E. Danieli, B. Blümich, *Applied Magnetic Resonance* 44 (1) (2013) 42–53.
- [48] G. Knothe, *Journal of American Oil Chemist' Society* 77 (5) (2000) 489–493.
- [49] O.I. Ece, F. Coban, *Clays and Clay Minerals* 42 (1) (1994) 81–92.
- [50] H. Yalcin, O. Bozkaya, *Clays and Clay Minerals* 43 (1995) 705–717.
- [51] S. Balci, *Journal of Chemical Technology and Biotechnology* 66 (1996) 72–78.
- [52] American Oil Chemists' Society, Official test method Cd 3a–63 for acid value, in *Official Methods and Recommended Practices of the American Oil Chemists' Society*, Champaign, Ill, 1998.
- [53] W. Xie, H. Peng, L. Chen, *Journal of Molecular Catalysis A: Chemical* 246 (2006) 24–32.
- [54] W. Xie, X. Huang, *Catalysis Letters* 107 (1–2) (2006) 53–59.
- [55] W. Xie, H. Peng, L. Chen, *Applied Catalysis A: General* 300 (2006) 67–74.
- [56] L.C. Meher, D. Vidya Sagar, S.N. Naik, *Renewable and Sustainable Energy Reviews* 10 (3) (2006) 248–268.
- [57] W. Zhou, S.K. Konar, G.B. Boock, *Journal of American Oil Chemist' Society* 80 (4) (2003) 367–371.
- [58] European Standard of EN 14103, Fat and Oil Derivatives – Fatty Acid Methyl Esters (FAME) – Determination of Ester and Linolenic Acid Methyl Ester Contents, April 2003.
- [59] J.B. Condon, *Surface Area and Porosity Determinations by Physisorption: Measurements and Theory*, Elsevier, Amsterdam, 2006.
- [60] G.W. Brindley, *The American Mineralogist* 44 (1959) 495–500.
- [61] S. Tunc, O. Duman, A. Cetinkaya, *Colloids and Surfaces A: Physicochemical Engineering Aspects* 377 (2011) 123–129.
- [62] <http://www.handbookofmineralogy.org/pdfs/sepiolite.pdf> (last visited 02.08.13).
- [63] M. Sánchez-Cantú, L.M. Pérez-Díaz, I. Pala-Rosas, E. Cadena-Torres, L. Juárez-Amador, E. Rubio-Rosas, M. Rodríguez-Acosta, J.S. Valente, *Fuel* 110 (2013) 54–62.
- [64] F. Jin, K. Kawasaki, H. Kishida, K. Tohji, T. Moriya, H. Enomoto, *Fuel* 86 (2007) 1201–1207.
- [65] European Standard of EN 14214, Automotive Fuels – Fatty Acid Methyl Esters (FAME) for Diesel Engines – Requirements and Test Methods, November 2008.
- [66] http://sdb.s.riond.b.aist.go.jp/sdb/cgi-bin/direct.frame_top.cgi, Spectral Database for Organic Compounds (SDBS) (last visited 02.08.13).
- [67] H. Liu, L. Su, Y. Shao, L. Zou, *Fuel* 97 (2012) 651–657.